Midazolam and Dexmedetomidine Affect Neuroglioma and Lung Carcinoma Cell Biology *In Vitro* and *In Vivo*

Chunyan Wang, M.D., Ph.D., Tanweer Datoo, M.Res., B.Sc., Hailin Zhao, Ph.D., Lingzhi Wu, M.Res., B.Sc., Akshay Date, M.B.B.S., Cui Jiang, M.Res., B.Sc., Robert D. Sanders, M.B.B.S., Ph.D., F.R.C.A., Guolin Wang, M.D., Ph.D., Charlotte Bevan, Ph.D., Daqing Ma, M.D., Ph.D., F.R.C.A.

ABSTRACT

Background: Several factors within the perioperative period may influence postoperative metastatic spread. Dexmedetomidine and midazolam are widely used general anesthetics during surgery. The authors assessed their effects on human lung carcinoma (A549) and neuroglioma (H4) cell lines *in vitro* and *in vivo*.

Methods: Cell proliferation and migration were measured after dexmedetomidine (0.001 to 10 nM) or midazolam (0.01 to 400 μM) treatment. Expression of cell cycle and apoptosis markers were assessed by immunofluorescence. Mitochondrial membrane potential and reactive oxygen species were measured by JC-1 staining and flow cytometry. Antagonists atipamezole and flumazenil were used to study anesthetic mechanisms of action. Tumor burden after anesthetic treatment was investigated with a mouse xenograft model of lung carcinoma.

Results: Dexmedetomidine (1 nM) promoted cell proliferation (2.9-fold in A549 and 2-fold in H4 cells *vs.* vehicle, $P < 0.0001$; n = 6), migration (2.2-fold in A549 and 1.9-fold in H4 cells *vs.* vehicle, $P < 0.0001$; n = 6), and upregulated antiapoptotic proteins *in vitro*. In contrast, midazolam (400 μM) suppressed cancer cell migration (2.6-fold in A549 cells, $P < 0.0001$; n = 4), induced apoptosis *via* the intrinsic mitochondrial pathway, decreased mitochondrial membrane potential, and increased reactive oxygen species expression *in vitro*—effects partly attributable to peripheral benzodiazepine receptor activation. Furthermore, midazolam significantly reduced tumor burden in mice (1.7-fold *vs.* control; $P < 0.05$; n = 6 per group).

Conclusions: Midazolam possesses antitumorigenic properties partly mediated by the peripheral benzodiazepine receptor, whereas dexmedetomidine promotes cancer cell survival through signaling *via* the α_2-adrenoceptor in lung carcinoma and neuroglioma cells. **(ANESTHESIOLOGY XXX; XXX:00-00)**

SURGICAL removal of primary tumors is often the first-line treatment for most cancers. Unfortunately, potentially curative surgical resection may paradoxically open a window of opportunity whereby residual cancer cells can overcome host defenses and become established as distant metastatic disease that can prove fatal.[1] The perioperative period has been established as a critical phase in influencing long-term cancer outcomes, with drugs used for general anesthesia implicated in affecting the behavior of tumor cells.[2–4]

Dexmedetomidine is a widely used sedative agent, with analgesic, sympatholytic, and anxiolytic effects during the perioperative period. It is a highly selective and potent α_2-adrenoceptor agonist with dose-dependent effects.[5] Dexmedetomidine has been shown to induce antiapoptotic effects through α_2-adrenoceptor signaling in neurons and immune cells, which are concerning for the use of the drug in the context of cancer.[6–9] Recent studies on the postoperative effect of dexmedetomidine on metastatic progression *in vivo* suggest that it is associated with reduced overall survival rates, although the molecular mechanisms that mediate this are not yet fully understood.[10,11]

Editor's Perspective

What We Already Know about This Topic

- Dexmedetomidine reduces cellular apoptosis, and it has been demonstrated previously that this antiapoptotic effect can not only increase cancer cell proliferation and migration but also reduce survival in experimental models of cancer growth.
- Midazolam has proapoptotic effects and can reduce cancer cell survival. The mechanisms by which midazolam suppresses cancer cell progression remain to be defined.

What This Article Tells Us That Is New

- As expected, dexmedetomidine enhanced cancer cell proliferation and migration, primarily by the upregulation of antiapoptotic proteins. By contrast, midazolam suppressed cancer cell proliferation and migration, induced mitochondria mediated apoptosis, and enhanced free radical production. These anticancer effects of midazolam, mediated by its activity at the peripheral benzodiazepine receptor, were achieved at high concentrations only.
- The data suggest that commonly used agents in the perioperative period may impact tumor cell growth; these effects have been demonstrated in preclinical studies, and therefore their relevance to clinical management of patients undergoing cancer surgery remains to be determined.

Supplemental Digital Content is available for this article. Direct URL citations appear in the printed text and are available in both the HTML and PDF versions of this article. Links to the digital files are provided in the HTML text of this article on the Journal's Web site

 Anesthesiology 2018; XXX:00-00

<zdoi;10.1097/ALN.0000000000002401>

The expression of α_2-adrenoceptors in breast cancer have been associated with increased tumor growth and migration both *in vitro* and *in vivo*, with activation of extracellular signal-related protein kinases by α_2-adrenoceptor agonists such as dexmedetomidine and clonidine shown to enhance this effect *in vitro* in breast cancer cells.[12–15] Inactivating α_2-adrenoceptor signaling inhibited the proliferation, migration, and invasion of breast cancers.[16] In lung alveolar epithelial cells, dexmedetomidine was found to protect against the effects of apoptosis induced by oxidative stress *in vitro* by enhancing cell survival and proliferation.[17] However, its functional and mechanistic effects have yet to be investigated in other types of cancers.

Midazolam is a widely used anesthetic from the benzodiazepine class, with a wide variety of uses including premedication, procedural sedation, and the treatment of insomnia and seizures. It exerts its action through benzodiazepine binding sites of the γ-aminobutyric acid type A ($GABA_A$) receptor, which mediates its primary clinical effects. Midazolam also binds peripheral benzodiazepine receptors, which tend to be localized to the outer mitochondrial membrane.[18,19]

Several types of cancers, including breast, ovarian, liver, and colon, show increased peripheral benzodiazepine receptor expression relative to healthy tissue.[20–22] In the breast cancer cell lines examined, expression of this receptor was relatively higher in the more aggressive phenotypes. Peripheral benzodiazepine receptors regulate various cellular functions including proliferation, oxidative processes, and apoptosis, highlighting their role in mitochondrial function.[18] Midazolam has been reported to activate the apoptotic extrinsic death receptor or intrinsic mitochondrial pathways to promote cellular apoptosis, but further underlying molecular mechanisms remain elusive.[23,24]

In the current work, we hypothesized that dexmedetomidine enhances cell proliferation, survival, and migration of human neuroglioma (H4) and lung carcinoma (A549) cell lines, whereas midazolam has apoptosis-inducing activity and suppresses cancer cell progression. We investigated changes in cell cycle and apoptotic markers, mitochondrial function, and cell signaling by α_2-adrenoceptors and benzodiazepine receptors, caused by dexmedetomidine and midazolam, respectively. The potential effect of dexmedetomidine and midazolam on tumor burden were also investigated in xenograft mice.

Materials and Methods

Cell Culture

Human lung carcinoma cells (A549) were obtained from the European Collection of Authenticated Cell Cultures (United Kingdom) and were authenticated by short-tandem repeat polymerase chain reaction DNA profiling. Human neuroglioma cells (H4) were a kind gift from Zhongcong Xie, M.D., Ph.D. (Massachusetts General Hospital, Boston, Massachusetts). H4 cells were purchased originally from and authenticated by the American Tissue Culture Collection by short-tandem repeat analysis. A549 and H4 cells were cultured at 37°C in a humidified atmosphere of 5% CO_2. A549 cells were maintained in Roswell Park Memorial Institute-1640 medium and H4 cells in Dulbecco's Modified Eagle Medium (Sigma-Aldrich, United Kingdom), supplemented with 10% fetal calf serum (HyClone, New Zealand), 1% L-glutamine, and 1% penicillin-streptomycin (Sigma-Aldrich). Cell morphology and behavior were closely monitored throughout the duration of study to ensure no phenotypic changes and contamination.

Interventions

Dexmedetomidine hydrochloride (Sigma-Aldrich) was used at concentrations of 0.001, 0.01, 0.1, 1, and 10 nM.[14] Midazolam (Sigma-Aldrich) was used at concentrations of 0.01, 0.1, 1, 10, 25, 50, 100, 200, and 400 μM.[25] Isotonic sodium chloride solution was used as the vehicle control for both anesthetics. The α_2-adrenoceptor antagonist atipamezole hydrochloride (Antisedan; Elanco Animal Health, United Kingdom) was used at a concentration of 10 nM, and the benzodiazepine receptor antagonist flumazenil (Sigma-Aldrich) was used at a concentration of 40 mM; antagonists were used at 10× greater concentrations, identified from our pilot studies, to ensure complete saturation of relevant receptors. Cells were exposed to antagonists for 10 min and then washed before addition of anesthetic agents in all combined experiments.

Cell Viability

Cell viability was assessed with colorimetric 3-(4,5-dimethylthiazol-2-yl)-2,5 diphenyl-2H-tetrazolium bromide assay (EMD Chemicals, USA). Culture medium was removed after incubation with or without indicated concentrations of drug. Cells in 24-well plates were treated with 500 μl 3-(4,5-dimethylthiazol-2-yl)-2,5 diphenyl-2H-tetrazolium bromide (0.5 mg/ml) and then incubated for 4 h under normal culture conditions. 3-(4,5-dimethylthiazol-2-yl)-2,5 diphenyl-2H-tetrazolium bromide was carefully removed; 500 μl of dimethyl sulfoxide

(www.anesthesiology.org). Preliminary data of the current work were presented in the Winter Anesthetic Research Society Meeting: The Royal College of Anaesthetists, London, United Kingdom, October 1 to 2, 2014 (https://doi.org/10.1093/bja/aeu367). C.W. and T.D. contributed equally to this article.

Submitted for publication November 1, 2017. Accepted for publication July 10, 2018. From the Department of Anesthesiology, Tianjin Medical University General Hospital, Tianjin, China (C.W., G.W.); Anaesthetics, Pain Medicine and Intensive Care, Department of Surgery and Cancer, Faculty of Medicine, Imperial College London, Chelsea and Westminster Hospital, London, United Kingdom (C.W., T.D., H.Z., L.W., A.D., C.J., D.M.); Tianjin Research Institute of Anesthesiology, Tianjin, China (C.W., G.W.); Department of Anesthesiology, University of Wisconsin, Madison, Wisconsin (R.D.S.); and Division of Cancer, Department of Surgery and Cancer, Faculty of Medicine, Imperial College London, Hammersmith Hospital, London, United Kingdom (C.B.).

(Fisher Scientific, United Kingdom) was added per well and then left for 10 min to allow dissolution of the crystals into a homogenous purple color. Forty microliters of this solution was transferred into a 96-well plate (VWR, United Kingdom), and a further 160 μl dimethyl sulfoxide was added. Absorbance was analyzed with a spectrophotometer (MRX Microplate Reader; Dynex Technologies, USA) at a wavelength of 595 nm. For additional experiments with midazolam at lower concentrations, cell viability was assessed using the Cell Counting Kit-8 assay. A549 and H4 cells were seeded into 96-well plates. Once confluent, cells were treated with 0.01, 0.1, 1, or 10 μM midazolam. Into each well, 10 μL of Cell Counting Kit-8 solution (Sigma-Aldrich) was added, and then the cells were incubated for 1 h under normal culture conditions. Absorbance was read at 450 nm with an ELx800 Microplate Reader (BioTek, USA). Cell viability was expressed relative to the control.

Wound-healing Assay

Cell migration was assessed with the wound-healing assay *in vitro*. Cells were cultured in 60-mm Petri dishes overnight to form a confluent monolayer. The scratch was performed on this monolayer with a 1-ml pipette tip under sterile conditions, after which interventions were added. After treatment, cells were washed twice with culture media. Images were taken with a digital camera (Canon, United Kingdom) immediately after addition of drugs, at 24 h, and at 48 h. Marks were made at the bottom of the dish to ensure that all images were taken at the same site. The area within the scratch occupied by cells at the different time points was calculated with Image-Pro Plus software (Media Cybernetics, USA). The percentage of gap closure was used as an indicator of cell migration.

Immunofluorescence Staining

A549 or H4 cells were fixed in 4% paraformaldehyde immediately after treatment and then blocked with 10% normal donkey serum (Sigma-Aldrich) for 1 h, followed by overnight incubation at 4°C in primary antibodies: mouse anti-Ki-67 (Dako, United Kingdom); anticyclin A; anticyclin D; anticyclin E; antiBcl-2; antiBcl-xL; antiBad; antimammalian target of rapamycin (Abcam, United Kingdom); rabbit anticleaved caspase 3, 8, or 9; anti-α_2-adrenoceptor; or antibenzodiazepine receptor (Abcam). Cells were washed with phosphate-buffered saline and then incubated in fluorescein isothiocyanate or rhodamine-conjugated secondary antibody (Merck Millipore, United Kingdom). Cells were counterstained and mounted with nuclear dye 4′, 6-diamidino-2-phenylindole–mounting medium (Vector Laboratories, USA). Images were captured under an Olympus BX4 microscope (United Kingdom). Fluorescent intensity was quantified with the mean pixel intensity of relevant antibody staining by ImageJ software (National Institutes of Health, USA). Ten representative regions per section were randomly selected by an assessor blinded to the treatment groups. Intensity values were calculated and expressed as relative to control.

Mitochondrial Membrane Potential Assay

JC-1 is a membrane-permeable dye used in apoptotic studies that exhibits potential-dependent accumulation in mitochondria, indicated by the shift from green fluorescent monomers to red fluorescent J-aggregates. A549 or H4 cells were cultured in 24-well plates at 37°C with or without anesthetic treatment. To each well, 100 μl of JC-1 staining solution (Abcam) per milliliter of culture medium was added. The solution was then gently agitated before incubation at 37°C in the dark for 15 min. Red fluorescent J-aggregates and green fluorescent JC-1 monomers were detected at excitation/emission wavelengths of 540/570 nm and 485/535 nm, respectively. Mitochondrial depolarization is indicated by a decrease in the red/green fluorescence intensity ratio.

Reactive Oxygen Species Measurement

Intracellular reactive oxygen species generation was detected by flow cytometry with the fluorescent dye dichlorodihydrofluorescein diacetate (Sigma-Aldrich). Cells were briefly washed twice with prewarmed Dulbecco's phosphate-buffered saline (Sigma-Aldrich). To stain cells, 10 μM dichlorodihydrofluorescein diacetate was added into a fluorescence-activated cell sorting tube in the dark for 30 min at 37°C. Immunofluorescence intensity was acquired and analyzed with flow cytometry (FACSCalibur; Becton Dickinson, USA). Each trial had at least 10,000 gated events.

Xenograft Model

Adult male BALB/C immunodeficient nude mice (Harlan, United Kingdom) were bred in temperature- and humidity-controlled cages in a specific pathogen-free facility at Chelsea and Westminster Campus, Imperial College London (United Kingdom). This study was approved by the Home Office, United Kingdom; all animal procedures were conducted in accordance with the United Kingdom Animals (Scientific Procedures) Act of 1986. A549 tumor cells (approximately 3.75×10^6) were suspended in 100 μl Roswell Park Memorial Institute-1640 media and injected subcutaneously into the middle left side of the mice. Four days after tumor cell implantation, mice were randomly selected and placed into one of three separate cages for treatment. Mice were treated daily for five days with saline, clinically relevant doses of midazolam (2.5 mg/kg per day), or dexmedetomidine (0.5 mg/kg per day) *via* subcutaneous injection in a different site to tumor implantation (n = 6 per group).[26] To ensure no cardiorespiratory disturbances by drug administration, each single dose of both sedatives given did not induce a sedative state to the animals. No statistical power calculation was conducted before the study given that the sample size was based on availability for this proof-of-concept study, and all data obtained have been reported. Three weeks after tumor implantation and treatment, mice were euthanized and underwent ascending aortic perfusion with 4% paraformaldehyde. Subdermal solid tumor masses were excised from mice and stored in 30% sucrose solution at 4°C to

allow dehydration. Tumor tissues were embedded in optimal cutting temperature solution (Tissue-Tek, Japan) and cryosectioned into 15μm thick sections. Frozen sections were blocked in 10% normal donkey serum at room temperature for 1 h and then incubated overnight at 4°C in primary antibodies: rabbit monoclonal cyclin-D1 antibody (Abcam) or rabbit polyclonal Ki67 antibody (Santa Cruz Biotechnology, USA). Slides were then incubated the following day in donkey antirabbit FITC (Merck Millipore) secondary antibody for 2 h at room temperature. Slides were counterstained and mounted with 4′, 6-diamidino-2-phenylindole–mounting medium and viewed under Olympus BX4 microscope.

Statistical Analysis

Data were first tested for normality with the Shapiro–Wilk test and then analyzed by one- or two-way ANOVA and Tukey *post hoc* test with GraphPad Prism (Version 7.0; GraphPad Software, USA). Only the following data were analyzed with two-way ANOVA: all cell viability assays and the wound-healing assay performed with dexmedetomidine in combination with inhibitor atipamezole. One-way ANOVA analysis factor was "treatment" between subjects. Two-way ANOVA analysis factors for the cell viability assays were "cell line" within subjects and "treatment" between subjects; for the wound-healing assay, factors were "time" within subjects and "treatment" between subjects. Data are presented as bar charts or scatter plots and expressed as mean ± SD. No outliers were detected and no data were excluded from the analysis. Differences with P value less than 0.05 were considered to be statistically significant.

Results

Dexmedetomidine Increases Cancer Cell Growth and Proliferation in a Dose-dependent Manner, Whereas Midazolam Decreases It

To examine whether dexmedetomidine and midazolam affect the growth of human lung carcinoma A549 cells and neuroglioma H4 cells, the 3-(4,5-dimethylthiazol-2-yl)-2,5 diphenyl-2H-tetrazolium bromide assay was used to measure cell viability. It was found that dexmedetomidine treatment for 24 h increased cell viability from concentrations as low as 0.001 nM (1.2-fold for both A549 [$P = 0.007$] and H4 cells [$P < 0.0001$] *vs.* vehicle) up to 10 nM (1.7-fold for A549 [$P < 0.0001$] and 1.6-fold for H4 cells [$P < 0.0001$] *vs.* vehicle; fig. 1A). However, midazolam treatment for 24 h decreased cell viability in a dose-dependent manner, from the highest concentration of 400 μM (2.6-fold for A549 and 1.9-fold for H4 cells *vs.* vehicle, $P < 0.0001$) down to 25 μM (1.2-fold for both A549 and H4 cells *vs.* vehicle, $P < 0.0001$; fig. 1B). Midazolam treatment at lower concentrations between 0.01 μM and 10 μM had no effect on cell viability, assessed using the Cell Counting Kit-8 assay (Supplemental Digital Content, fig. S1, http://links.lww.com/ALN/B760). To further investigate whether the observed changes in cell viability were due to cell death or proliferation, Ki67 expression was assessed through immunofluorescence staining in A549 and H4 cells treated with 1 nM dexmedetomidine (fig. 1, C and D) or 400 μM midazolam (fig. 1, E and F). The Ki67 protein is strictly associated with cellular proliferation and is present during all active phases of the cell cycle. Dexmedetomidine increased Ki67 expression in both A549 and H4 cells (2.9- and 2-fold, respectively, *vs.* vehicle, $P < 0.0001$). However, midazolam decreased Ki67 expression (1.7-fold for A549 [$P < 0.0001$] and 1.4-fold for H4 cells [$P = 0.0003$] *vs.* vehicle).

Dexmedetomidine Enhances but Midazolam Decreases Cancer Cell Migration

The effects of dexmedetomidine treatment on migration of A549 and H4 cells, and of midazolam on cell migration of A549 cells, were assessed with the wound-healing assay (fig. 2). Our results indicate that migration of both cell lines is enhanced by dexmedetomidine (by 2.2-fold in A549 and 1.9-fold in H4 cells *vs.* vehicle, $P < 0.0001$) but decreased by midazolam (by 2.6-fold in A549 cells *vs.* vehicle, $P < 0.0001$).

Dexmedetomidine Promotes Cell Cycling, Whereas Midazolam Inhibits It by Affecting Cyclin A, D, and E Expression

To observe which aspects of the cell cycle are affected by dexmedetomidine and midazolam, A549 and H4 cells treated with the two agents were stained for cyclin A (fig. 3), D, and E (Supplemental Digital Content, fig. S2, http://links.lww.com/ALN/B761, and S3, http://links.lww.com/ALN/B762). Similar trends were observed for all three markers, with dexmedetomidine increasing expression compared with the vehicle control: cyclin A by at least 1.8-fold in both cell lines, cyclin D by 1.8- and 2.2-fold in A549 and H4 cells, respectively, and cyclin E by 2.6- and 2.1-fold in A549 and H4 cells, respectively. In contrast, midazolam decreased cyclin expression compared with the vehicle control: cyclin A by 1.4- and 1.5-fold in A549 and H4 cells, respectively, cyclin D by 1.5-fold in both cell lines, and cyclin E by 1.6-fold in both cell lines. All observations were statistically significant ($P < 0.001$).

Midazolam Induces Apoptosis through Activation of the Intrinsic Mitochondrial Pathway

As previously observed, dexmedetomidine and midazolam affected cell viability differently. The effects of both agents on cell death were first investigated through immunofluorescence staining of antiapoptotic proteins Bcl-2 and Bcl-xL in H4 cells (Supplemental Digital Content, fig. S4, http://links.lww.com/ALN/B763). Dexmedetomidine increased expression of Bcl-2 and Bcl-xL (2.9- and 2.4-fold, respectively, *vs.* vehicle, $P < 0.0001$), whereas midazolam decreased expression of both Bcl-2 ($P = 0.0002$) and Bcl-xL ($P = 0.002$) by 1.6-fold compared with the vehicle. To corroborate this and identify the cell death response involved, we evaluated concentrations of cleaved caspases 3, 8, and 9. No differences in

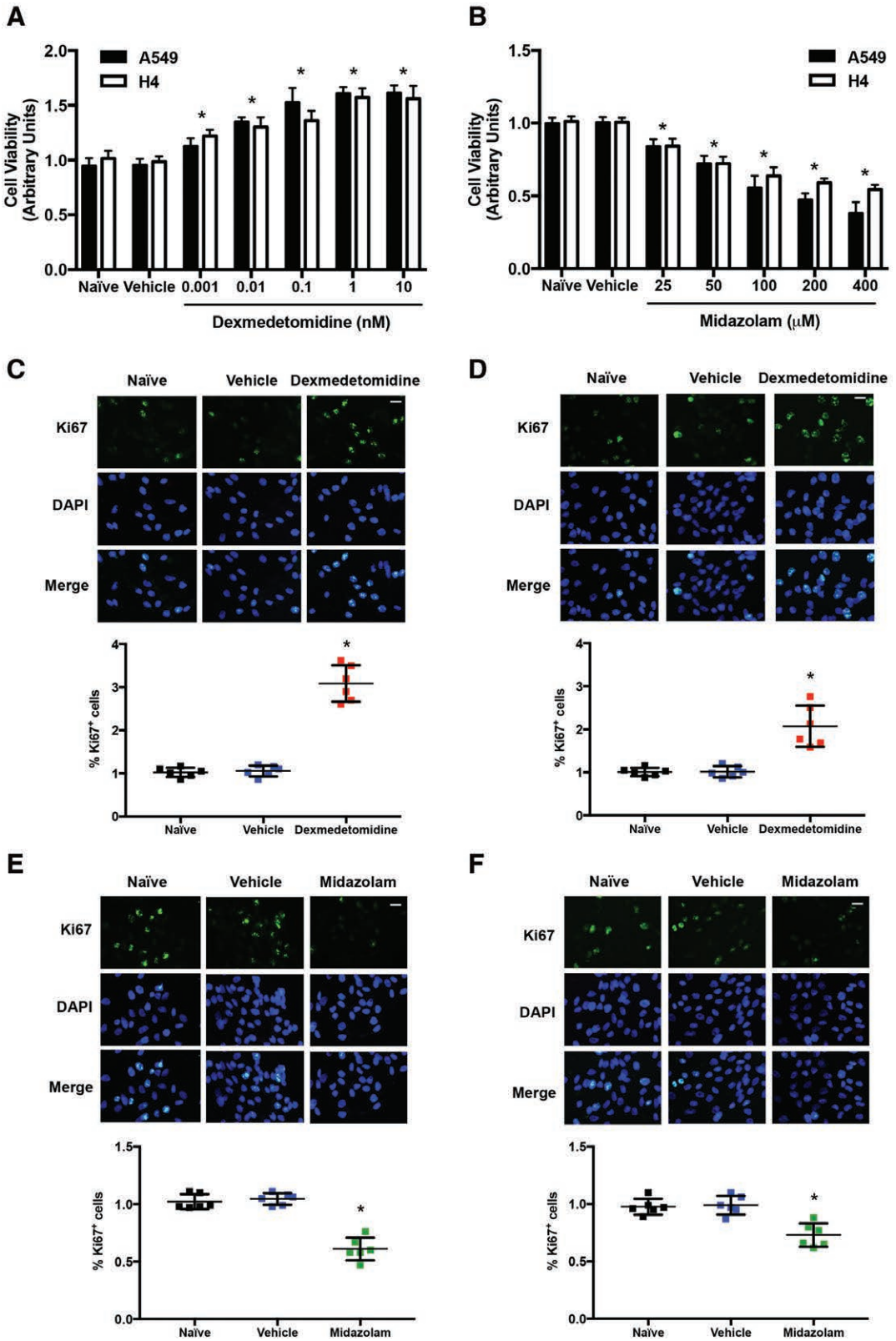

Fig. 1. Effect of dexmedetomidine and midazolam on growth and proliferation of A549 and H4 cells. Cells were treated with increasing concentrations of (*A*) dexmedetomidine (0.001 to 10 nM) or (*B*) midazolam (25 to 400 μM) for 24 h, then cell viability was determined by 3-(4,5-dimethylthiazol-2-yl)-2,5 diphenyl-2H-tetrazolium bromide assay. Representative images and quantification of immunofluorescence staining of Ki67$^+$ cells after 24 h treatment with 1 nM dexmedetomidine of A549 (*C*) and H4 (*D*) cells or 400 μM midazolam treatment of A549 (*E*) and H4 cells (*F*). Data are presented as mean ± SD. *P < 0.01 *versus* vehicle. n = 6 independent experiments. *Scale bar*: ×20 magnification, 50 μm.

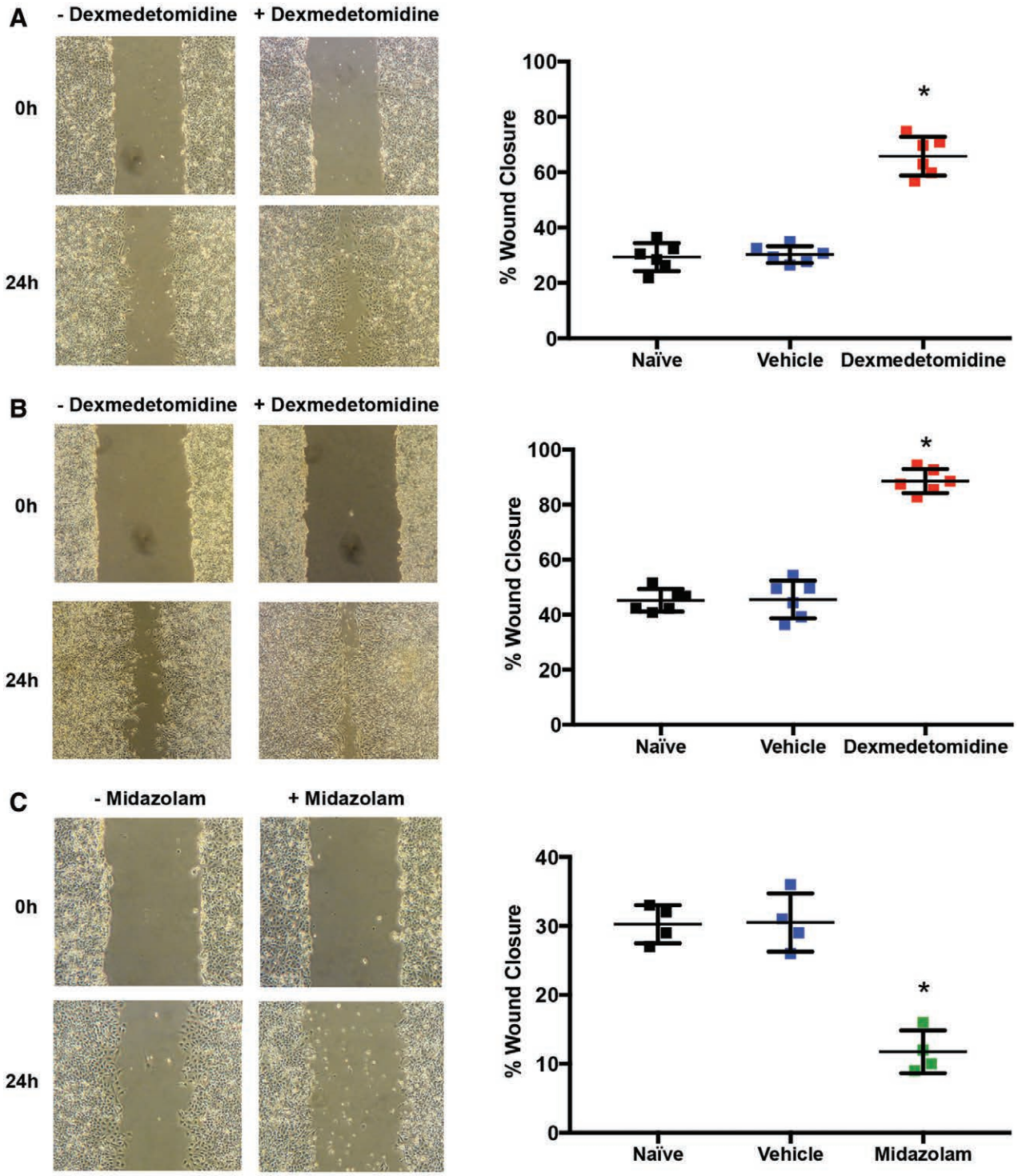

Fig. 2. Effect of dexmedetomidine and midazolam on migration of A549 and H4 cells. Cell migration was measured by wound-healing assay after 24 h treatment with 1 nM dexmedetomidine of A549 (*A*) or H4 (*B*) cells; *n* = 6 independent experiments. Cell migration of A549 cells was also assessed after 24 h treatment with 400 μM midazolam (*C*); *n* = 4 independent experiments. Data are presented as mean ± SD. **P* < 0.01 *versus* vehicle.

any caspases were detected with dexmedetomidine treatment (Supplemental Digital Content, fig. S5, http://links.lww.com/ALN/B764, and S6, http://links.lww.com/ALN/B765). It is interesting that midazolam caused the activation of caspases 3 and 9 (fig. 4), but not caspase 8 (Supplemental Digital Content, fig. S6, http://links.lww.com/ALN/B765), suggesting stimulation of the intrinsic mitochondrial apoptotic pathway. Reactive oxygen species, cytochrome C, and Bad play

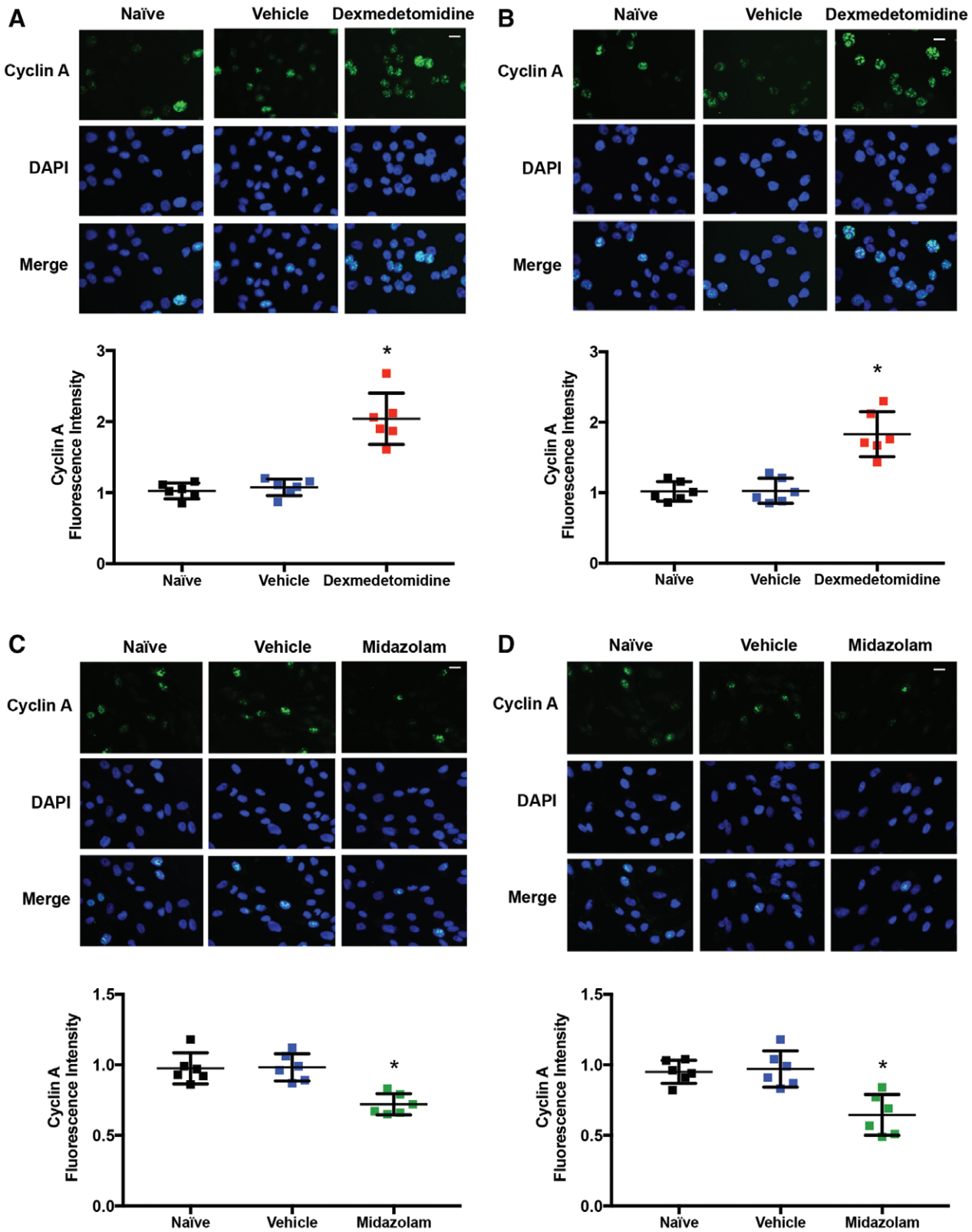

Fig. 3. Effect of dexmedetomidine and midazolam on cyclin A expression of A549 and H4 cells. Representative images and quantification of immunofluorescence staining of cyclin A^+ cells after 24 h treatment with 1 nM dexmedetomidine of A549 (*A*) and H4 (*B*) cells or 400 μM midazolam treatment of A549 (*C*) and H4 cells (*D*). Data are presented as mean ± SD. *$P < 0.01$ *versus* vehicle. $n = 6$ independent experiments. *Scale bar*: ×20 magnification, 50 μm.

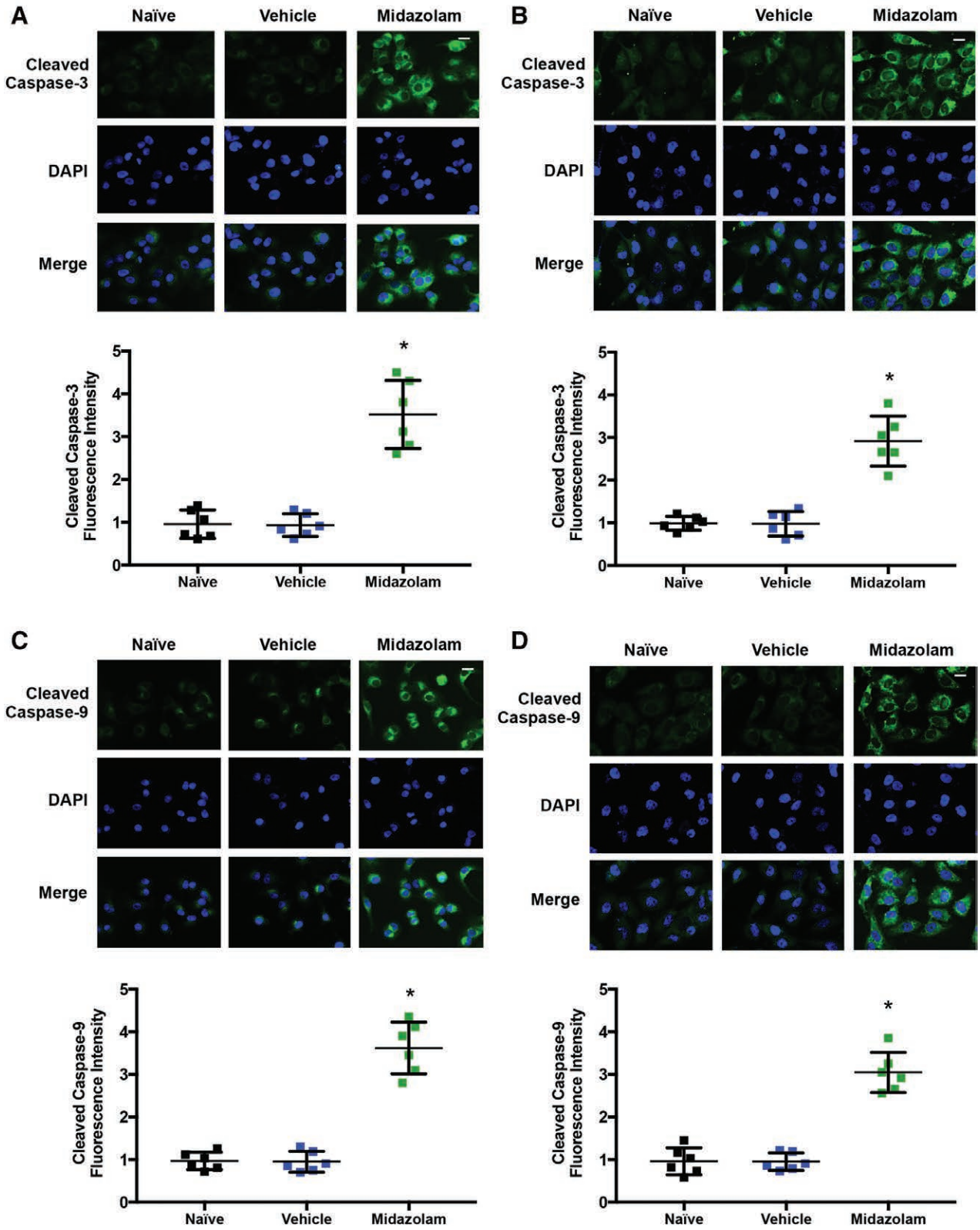

Fig. 4. Effect of midazolam on cleaved caspase 3 and caspase 9 expression of A549 and H4 cells. Representative images and quantification of immunofluorescence staining of cleaved caspase 3^+ A549 (*A*) or H4 (*B*) cells and cleaved caspase 9^+ A549 (*A, C*) or H4 (*B, D*) cells after 24 h treatment with 400 μM midazolam treatment. Data are presented as mean ± SD. $^*P < 0.01$ *versus* vehicle. *n* = 6 independent experiments. *Scale bar*: ×20 magnification, 50 μm.

an important role in this pathway. Intracellular concentrations of reactive oxygen species were measured in both A549 and H4 cells after midazolam treatment with flow cytometry, and it was found that midazolam treatment increased reactive oxygen species concentrations in A549 ($P = 0.0003$) and H4 ($P = 0.0002$) cell lines by at least 1.1-fold compared with the vehicle treatment (fig. 5, A and B). Cytochrome C and Bad were also found to increase after midazolam treatment in H4 cells (2.3- and 2.5-fold, respectively, *vs.* vehicle, $P < 0.0001$; Supplemental Digital Content, fig. S7, http://links.lww.com/ALN/B766). In addition, midazolam caused depolarization of the mitochondrial membrane, as reflected by the decreased amount of J-aggregates (red fluorescent staining) compared with JC-1 monomers (green fluorescence), indicated by a lower red/green ratio compared with the vehicle control in A549 (2.3-fold, $P = 0.0004$) and H4 cells (3.2-fold, $P = 0.0005$; fig. 5, C and D).

Dexmedetomidine Exerts Its Action via the α_2-Adrenoceptor and Midazolam Partly through the Peripheral Benzodiazepine Receptor

For the purpose of understanding the specificity of dexmedetomidine and midazolam and their actions *via* the α_2-adrenoceptor and benzodiazepine receptor, respectively, studies were carried out with atipamezole, a synthetic α_2-adrenoceptor antagonist, and flumazenil, a benzodiazepine receptor antagonist. The presence of these receptors was first confirmed in both A549 and H4 cell lines (Supplemental Digital Content, fig. S8, http://links.lww.com/ALN/B767, and fig. S9, http://links.lww.com/ALN/B768). It was found that atipamezole could reduce dexmedetomidine-enhanced cell migration of A549 cells at 24 h and 48 h to baseline concentration (Supplemental Digital Content, fig. S8B, http://links.lww.com/ALN/B767). Atipamezole was also able to decrease the cell viability-promoting effects of dexmedetomidine, although atipamezole alone increased cell viability of both A549 and H4 cells (Supplemental Digital Content, fig. S8C, http://links.lww.com/ALN/B767). Further to this, atipamezole alone had no effect on cyclin A or D expression. However, it partially reduced dexmedetomidine-enhanced cyclin A and D expressions (Supplemental Digital Content, fig. S8D and S8E, http://links.lww.com/ALN/B767). Dexmedetomidine also significantly increased mammalian target of rapamycin expression in A549 cells by 1.5-fold compared with the vehicle control ($P = 0.0006$; Supplemental Digital Content, fig. S7C, http://links.lww.com/ALN/B766). However, flumazenil alone had no effect on cell viability and Ki67 expression but partially reversed the decreases in cell viability and Ki67 expression caused by midazolam treatment in both A549 and H4 cells (Supplemental Digital Content, fig. S9, http://links.lww.com/ALN/B768).

Midazolam Significantly Reduces A549 Tumor Growth, Ki67, and Cyclin D Expression In Vivo

To extrapolate our *in vitro* findings to an *in vivo* setting, we treated nude mice implanted with A549 tumors with saline, dexmedetomidine, or midazolam. No differences in animal weight were detected before euthanizing the mice (fig. 6A); however, midazolam significantly reduced tumor size compared with tumors from naïve animals (fig. 6, B and C). Tumor tissue sections stained for Ki67 (fig. 6D) and cyclin D (fig. 6E) showed a decrease in both protein expressions in midazolam-treated animals and an increase in both markers in dexmedetomidine-treated animals, compared with animals without treatment. We noted that three weeks after tumor implantation, two of six dexmedetomidine-treated mice developed skin ulcers on the xenograft and reached clinical endpoints evaluated with a well-established scoring system.

Discussion

In the present study, dexmedetomidine enhanced the proliferation and migration of A549 and H4 cells *in vitro via* adrenergic signaling and upregulation of antiapoptotic proteins Bcl-2 and Bcl-xL. In contrast, midazolam suppressed cancer cell proliferation and migration, induced apoptosis *via* the intrinsic mitochondrial pathway, caused mitochondrial depolarization, and increased intracellular reactive oxygen species *in vitro*. Midazolam reduced tumor burden, Ki67 expression, and cyclin D expression *in vivo*. Although dexmedetomidine did not affect tumor growth *in vivo* in this particular scenario, Ki67 and cyclin D expression were both found to be upregulated in extracted tumor tissue.

The effects of adrenergic signaling in breast cancer have been reported, and our study on dexmedetomidine suggests that these effects may extend to other cancer types.[14,27,28] Midazolam has been identified to have apoptosis-inducing effects in several cancer cell lines *in vitro,* including MA-10 Leydig cells, lymphoma, neuroblastoma, and leukemia.[24,25,29] We found that dexmedetomidine increased, and midazolam decreased, A549 and H4 cell viability in a dose-dependent manner. We consistently observed an increase in Ki67 and cyclin A, D, and E expression after dexmedetomidine treatment. Ki67 is present during all phases of the cell cycle (G_1, S, G_2, and mitosis) but absent from resting cells (G_O), providing a reliable marker of growth.[30] Cyclins regulate cell cycle progression, each protein associated with a different stage of the cycle. A consistent up- or downregulation in Ki67 and all cyclins assessed in this study shows the broad rather than specific effects of the drug treatment on the cell cycle. Atipamezole, an α_2-adrenoceptor antagonist, reversed the effects of dexmedetomidine on cell proliferation and migration entirely but only partially reduced cyclin A and D induction. This suggests that dexmedetomidine may influence pathways other than that activated by α_2-adrenoceptors. Flumazenil partially reversed midazolam-induced decreases in cell viability and proliferation. Flumazenil is a specific competitive antagonist at benzodiazepine receptors associated with receptors for $GABA_A$, indicating that midazolam effects were partly mediated by the benzodiazepine binding site of $GABA_A$ or peripheral benzodiazepine

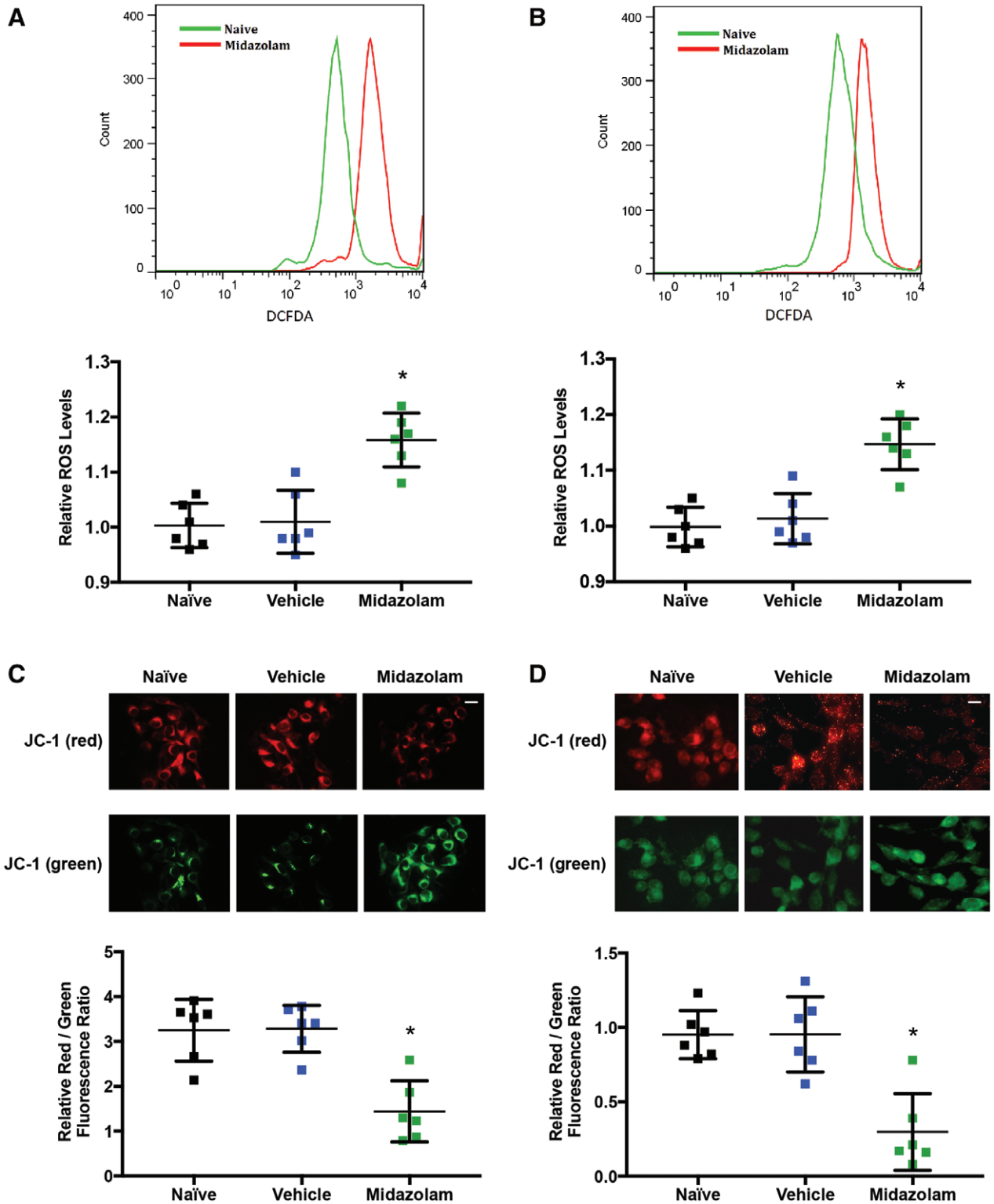

Fig. 5. Effect of midazolam on intracellular reactive oxygen species concentrations and mitochondrial membrane potential. Intracellular reactive oxygen species concentrations were measured in A549 (*A*) and H4 (*B*) cells after 24 h treatment with 400 μM midazolam by flow cytometry. Representative images and quantification of immunofluorescence staining of A549 (*C*) and H4 (*D*) cells after 24 h treatment with 400 μM midazolam for J-aggregates (*red fluorescence*) and JC-1 monomers (*green fluorescence*). Data are presented as mean ± SD. **P* < 0.01 *versus* vehicle. *n* = 6 independent experiments. *Scale bar*: ×20 magnification, 50 μm. DCFDA, dichlorodihydrofluorescein diacetate.

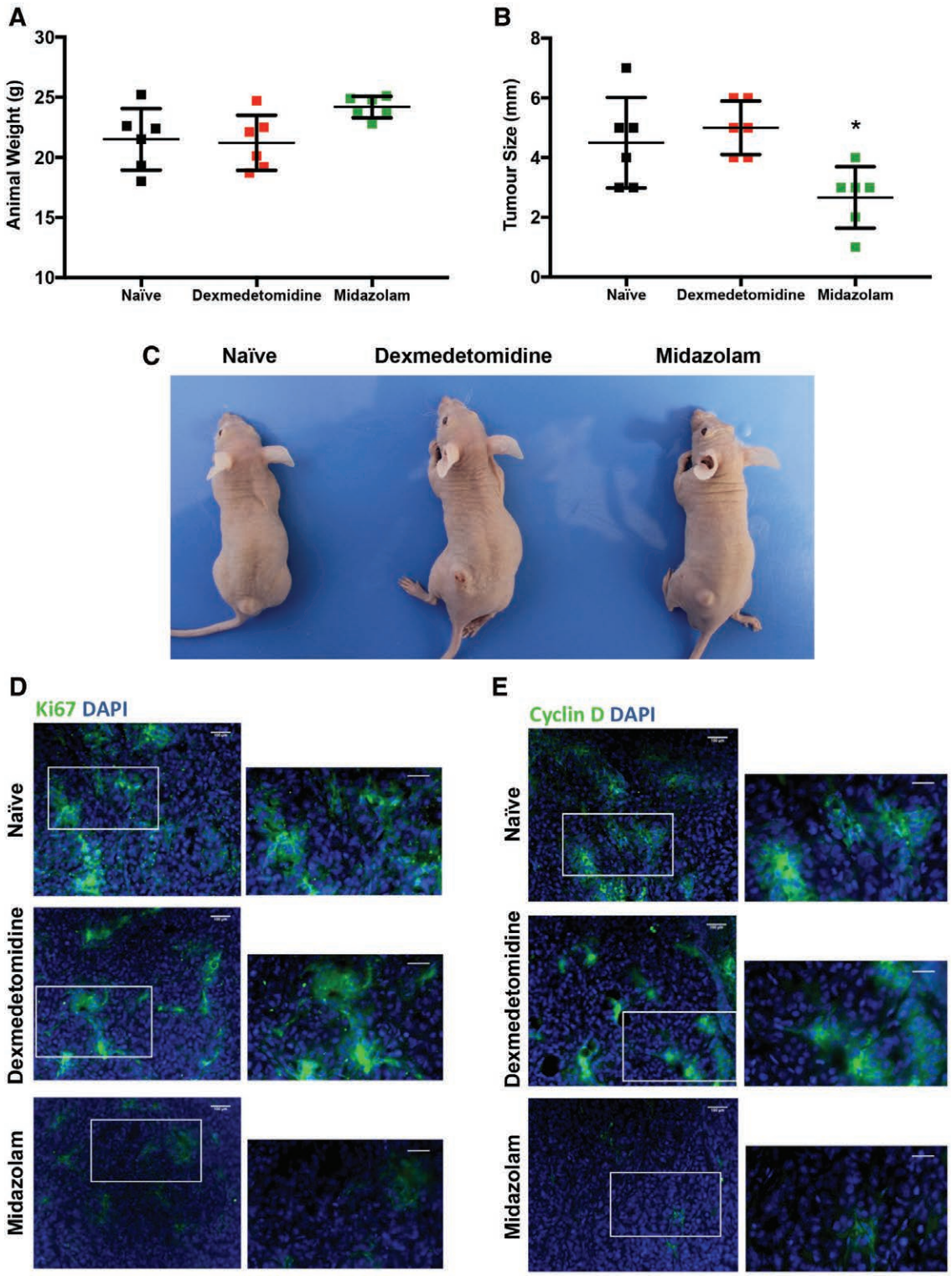

Fig. 6. Effects of dexmedetomidine and midazolam on A549 tumors *in vivo*. Mice with A549 tumors were treated daily for five days with saline, dexmedetomidine (0.5 mg/kg per day), or midazolam (2.5 mg/kg per day) *via* subcutaneous injection. No differences in animal weight (*A*) were detected, but midazolam significantly decreased tumor size (*B*). Representative photos taken of a mouse from each group before euthanasia; two of six mice treated with dexmedetomidine were observed to have red spots or scarring on tumor (*C*). Representative images of immunofluorescence staining of Ki67 (*D*) and cyclin D (*E*) from tumor sections showed an increase in both proteins in dexmedetomidine-treated mice and a decrease in midazolam-treated mice. Data are presented as mean ± SD. *$P < 0.05$ *versus* naïve control. $n = 6$ mice per group. *Scale bar*: ×10 magnification, 100 μm; ×20 magnification, 50 μm.

receptors.[31] Indeed, our data clearly show that benzodiazepine receptors exist in both A549 and H4 cell lines. Other mechanisms, including intracellular acidosis induced by benzodiazepines, may also contribute to the "killing" effect of midazolam.[32]

The two main pathways of apoptosis for cells are extrinsic or intrinsic. The extrinsic pathway is initiated by the death receptor, activating the death-inducing signaling complex and then caspase 8. The intrinsic pathway requires permeabilization of the mitochondria and release of cytochrome C, initiating the caspase cascade by activating caspase 9. This pathway can be triggered by cytochrome C and reactive oxygen species.[33,34] Both pathways converge onto effector caspase 3.[35] Here, midazolam induced apoptosis in both A549 and H4 cells through the intrinsic pathway, demonstrated by upregulated cleaved caspase 9 and 3, but not cleaved caspase 8, in addition to increased concentrations of cytochrome C and reactive oxygen species.

In cancer cells, high concentrations of reactive oxygen species are produced due to various factors such as increased metabolic activity, mitochondrial dysfunction, and cellular signaling. Reactive oxygen species can enhance cellular proliferation and migration and induce DNA damage that potentiates tumorigenesis. However, they can also induce cellular senescence and cell death. Reactive oxygen species production by carcinoma cells tends to be elevated *in vitro* and *in vivo*.[36] Midazolam has previously been shown to induce apoptosis possibly through the suppression of reactive oxygen species production in K562 human leukemia cells.[24] Our study, however, showed midazolam increased reactive oxygen species in both A549 and H4 cells. Excessive concentrations of intracellular reactive oxygen species can induce cell cycle arrest, senescence, apoptosis, and even uncontrolled cell death.[34,37,38] Increased mitochondrial oxidative stress causes cytochrome C release, the activation of caspases, and cell death, all observed in this study.[34,39] Mitochondrial release of free radicals leads to activation of the c-Jun N-terminal kinase signaling pathway. Upon reactive oxygen species stimulation, c-Jun N-terminal kinases phosphorylate and cause the downregulation of antiapoptotic proteins including Bcl-2 and Bcl-xL, both of which have been shown to protect cells from apoptosis induced by reactive oxygen species.[39–41] Our data collectively suggest that midazolam stimulates the intrinsic mitochondrial pathway, through a disproportional increase in reactive oxygen species.

Although midazolam is more widely reported to act *via* the $GABA_A$ receptor, our data show midazolam caused mitochondrial depolarization in both cell lines investigated, supporting the notion that midazolam also acts *via* peripheral benzodiazepine receptors on the outer mitochondrial membrane.[18,19] These receptors are part of the mitochondrial permeability transition pore, located at the contact site between the inner and outer mitochondrial membranes.[42] The opening of this pore is a critical event during apoptosis and can be triggered by pseudopathologic conditions of oxidative stress *in vitro*.[43] Partial permeabilization of the inner mitochondrial membrane leads to an abrupt loss in transmembrane potential, whereas complete permeabilization of the outer mitochondrial membrane results in leakage of potentially toxic intermembrane proteins that result in apoptosis.[44] Endozepine, the endogenous ligand of peripheral benzodiazepine receptors, released from damaged mitochondria may theoretically act on intact mitochondria, participating in a positive feedback loop to accelerate the induction of mitochondrial membrane permeabilization.[45,46] Thus, we suggest two potential mechanisms for the action of midazolam as observed in this study: midazolam may bind to the peripheral benzodiazepine receptors located on the mitochondria to stimulate cellular apoptosis and/or may trigger the opening of the mitochondrial permeability transition pore to induce apoptosis by increasing intracellular reactive oxygen species. These hypotheses certainly warrant further studies.

Dexmedetomidine increased cancer cell survival by modulating Bcl-2 and Bcl-xL expression. Cancer cells often upregulate antiapoptotic Bcl-2 proteins as a protective mechanism against apoptosis, preventing mitochondrial outer membrane permeabilization.[33] Overexpression of Bcl-2 alone is not oncogenic, but it can dramatically enhance tumorigenesis in combination with other growth-promoting oncogenes such as Myc.[47] Further to this, we observed an increase in mammalian target of rapamycin expression, showing the potential of dexmedetomidine to perturb cellular signaling. The mechanism of α_2-adrenergic receptors includes the activation of inhibitory G-proteins or modulation of ion channel activity, although its effects on specific signaling pathways are still unclear.[48] The phosphoinositide-3-kinase/Akt/mammalian target of rapamycin pathway is critical in the regulation of numerous cellular functions including proliferation, survival, and differentiation and is one of the most activated pathways in cancers.[49] Mammalian target of rapamycin is a serine/threonine kinase that monitors nutrient availability, cellular oxygen and energy levels, and mitogenic signals.[50] Dexmedetomidine increases phosphorylated Akt and mammalian target of rapamycin concentrations as a mechanism of inhibiting neuronic autophagy.[51] In a previous study, we found that dexmedetomidine could reverse the downregulation of phosphorylated mammalian target of rapamycin in lung alveolar epithelial cell injury induced by hydrogen peroxide.[17] In this study, we observed prolonged dexmedetomidine treatment alone could increase mammalian target of rapamycin expression in the same cell line. Thus, dexmedetomidine can promote tumorigenesis through more than one mechanism including enhancing cell cycle progression and cell survival; however, further work is required on its effects on cancer cell signaling pathways.

In line with our *in vitro* data, our *in vivo* work shows that midazolam treatment reduces tumor size, Ki67 expression, and cyclin D expression in mice. Dexmedetomidine increased the expression of both these proteins, but surprisingly, we did not observe any significant effects on tumor

size. A recent *in vivo* study found that dexmedetomidine administered by a slow release vehicle, maintaining prolonged exposure to the drug, increased tumor cell retention and growth of metastasis of breast, lung, and colon cancer cells in rodent models.[11] It is likely that the living duration (three weeks) given to mice after tumor implantation in our study was not sufficient to allow any significant changes in tumor growth caused by the treatment regime given. The reason this duration was set up is because the tumor burden in mice treated with dexmedetomidine caused severe whole body physiologic deterioration in at least two animals and with animal welfare in mind, all animals were euthanized at the end of the third week after tumor implantation, limiting our *in vivo* study.

Another limitation of this study appears to be the high doses used for treatment. Although the midazolam and dexmedetomidine doses used in our experiments have been reported in previous *in vitro* studies, caution needs to be taken when interpreting this data, as experimental *in vitro* and *in vivo* conditions cannot accurately represent clinical conditions.[14,24,25,52] The clinical concentrations for dexmedetomidine range from 0.2 to 2 ng/ml (1 to 10 nM), and the concentrations used in this study correspond well with these.[53,54] By contrast, clinical concentrations of midazolam range from 100 to 200 ng/ml (less than 1 μM); the concentrations used here are considerably greater (25 to 400 μM) than those achieved in the clinical setting.[55] Our cell viability data at nM concentration range did not show any effects of midazolam on either cell line (Supplemental Digital Content, fig. S1, http://links.lww.com/ALN/B760), indicating that midazolam only stimulated apoptosis at concentrations higher than those achieved clinically. These data somewhat highlight the differences between the growth-promoting effect of dexmedetomidine and the lack of effect of midazolam on tumor cell growth at clinically relevant concentrations.

In conclusion, midazolam inhibited cellular proliferation and induced apoptosis through the intrinsic mitochondrial pathway in human lung carcinoma and neuroglioma cells, effects that may be in part mediated by peripheral benzodiazepine receptors. Midazolam also inhibited lung tumor growth in xenograft mice. Dexmedetomidine, however, increased cellular proliferation, migration, and survival through, but not restricted to, pathways activated by α_2-adrenoceptors. Although our study would benefit from deeper investigation into specific receptor activation and cellular signaling, the work reported here furthers the current understanding of the mechanisms of action of dexmedetomidine and midazolam on cancer cells.

Acknowledgments

The authors sincerely thank Prof. Zhongcong Xie, M.D, Ph.D. (Massachusetts General Hospital, Boston, Massachusetts), for his kind gift of the H4 cell line used in these studies.

Research Support

The project was supported by a grant from the British Oxygen Company Chair (to Prof. Ma), Royal College of Anaesthetists (London, United Kingdom); European Cooperation in Science and Technology Action (CA15204; Brussels, Belgium; to Prof. Ma); and grant 81600962 (to Dr. Chunyan Wang) from the National Natural Science Foundation (Beijing, China). Dr. Chunyan Wang also received a scholarship (2016041) from the China Scholarship Committee (Beijing, China). Tanweer Datoo received a president's Ph.D. scholarship from Imperial College London (United Kingdom).

Competing Interests

The authors declare no competing interests.

Correspondence

Address correspondence to Prof. Ma: Anaesthetics, Pain Medicine and Intensive Care, Department of Surgery and Cancer, Faculty of Medicine, Imperial College London, Chelsea and Westminster Hospital, London, United Kingdom. d.ma@imperial.ac.uk.

References

1. Demicheli R, Retsky MW, Hrushesky WJ, Baum M, Gukas ID: The effects of surgery on tumor growth: A century of investigations. Ann Oncol 2008; 19:1821–8
2. Horowitz M, Neeman E, Sharon E, Ben-Eliyahu S: Exploiting the critical perioperative period to improve long-term cancer outcomes. Nat Rev Clin Oncol 2015; 12:213–26
3. Wigmore TJ, Mohammed K, Jhanji S: Long-term survival for patients undergoing volatile *versus* IV anesthesia for cancer surgery: A retrospective analysis. ANESTHESIOLOGY 2016; 124:69–79
4. Huang H, Benzonana LL, Zhao H, Watts HR, Perry NJ, Bevan C, Brown R, Ma D: Prostate cancer cell malignancy via modulation of HIF-1α pathway with isoflurane and propofol alone and in combination. Br J Cancer 2014; 111:1338–49
5. Kaur M, Singh PM: Current role of dexmedetomidine in clinical anesthesia and intensive care. Anesth Essays Res 2011; 5:128–33
6. Sanders RD, Xu J, Shu Y, Januszewski A, Halder S, Fidalgo A, Sun P, Hossain M, Ma D, Maze M: Dexmedetomidine attenuates isoflurane-induced neurocognitive impairment in neonatal rats. ANESTHESIOLOGY 2009; 110:1077–85
7. Sanders RD, Sun P, Patel S, Li M, Maze M, Ma D: Dexmedetomidine provides cortical neuroprotection: Impact on anaesthetic-induced neuroapoptosis in the rat developing brain. Acta Anaesthesiol Scand 2010; 54:710–6
8. Ma D, Hossain M, Rajakumaraswamy N, Arshad M, Sanders RD, Franks NP, Maze M: Dexmedetomidine produces its neuroprotective effect via the alpha 2A-adrenoceptor subtype. Eur J Pharmacol 2004; 502:87–97
9. Qiao H, Sanders RD, Ma D, Wu X, Maze M: Sedation improves early outcome in severely septic Sprague Dawley rats. Crit Care 2009; 13:R136
10. Lavon H, Krigman R, Elbaz E, Sorski L, Matzner P, Shaashua L, Benbenishty A, Cata JP, Gottumukkala V, Ben-Eliyahu S: The perioperative use of the sedative dexmedetomidine in cancer patients may have detrimental effects. Brain Behav Immun 2015; 49, Supplement: e29

11. Lavon H, Matzner P, Benbenishty A, Sorski L, Rossene E, Haldar R, Elbaz E, Cata JP, Gottumukkala V, Ben-Eliyahu S: Dexmedetomidine promotes metastasis in rodent models of breast, lung, and colon cancers. Br J Anaesth 2018; 120:188–96
12. Pérez Piñero C, Bruzzone A, Sarappa MG, Castillo LF, Lüthy IA: Involvement of α2- and β2-adrenoceptors on breast cancer cell proliferation and tumour growth regulation. Br J Pharmacol 2012; 166:721–36
13. Vázquez SM, Mladovan AG, Pérez C, Bruzzone A, Baldi A, Lüthy IA: Human breast cell lines exhibit functional alpha2-adrenoceptors. Cancer Chemother Pharmacol 2006; 58:50–61
14. Castillo LF, Rivero EM, Goffin V, Lüthy IA: Alpha2-adrenoceptor agonists trigger prolactin signaling in breast cancer cells. Cell Signal 2017; 34:76–85
15. Xia M, Ji NN, Duan ML, Tong JH, Xu JG, Zhang YM, Wang SH: Dexmedetomidine regulate the malignancy of breast cancer cells by activating α2-adrenoceptor/ERK signaling pathway. Eur Rev Med Pharmacol Sci 2016; 20:3500–6
16. Xia M, Tong JH, Zhou ZQ, Duan ML, Xu JG, Zeng HJ, Wang SH: Tramadol inhibits proliferation, migration and invasion via α2-adrenoceptor signaling in breast cancer cells. Eur Rev Med Pharmacol Sci 2016; 20:157–65
17. Cui J, Zhao H, Wang C, Sun JJ, Lu K, Ma D: Dexmedetomidine attenuates oxidative stress induced lung alveolar epithelial cell apoptosis *in vitro*. Oxid Med Cell Longev 2015; 2015:358396
18. Casellas P, Galiegue S, Basile AS: Peripheral benzodiazepine receptors and mitochondrial function. Neurochem Int 2002; 40:475–86
19. Olkkola KT, Ahonen J: Midazolam and other benzodiazepines. Handb Exp Pharmacol 2008; 182:335–60
20. Hunakova L, Bodo J, Chovancova J, Sulikova G, Pastorekova S, Sedlak J: Expression of new prognostic markers, peripheral-type benzodiazepine receptor and carbonic anhydrase IX, in human breast and ovarian carcinoma cell lines. Neoplasma 2007; 54:541–8
21. Venturini I, Alho H, Podkletnova I, Corsi L, Rybnikova E, Pellicci R, Baraldi M, Pelto-Huikko M, Helén P, Zeneroli ML: Increased expression of peripheral benzodiazepine receptors and diazepam binding inhibitor in human tumors sited in the liver. Life Sci 1999; 65:2223–31
22. Katz Y, Eitan A, Gavish M: Increase in peripheral benzodiazepine binding sites in colonic adenocarcinoma. Oncology 1990; 47:139–42
23. Yon JH, Daniel-Johnson J, Carter LB, Jevtovic-Todorovic V: Anesthesia induces neuronal cell death in the developing rat brain via the intrinsic and extrinsic apoptotic pathways. Neuroscience 2005; 135:815–27
24. Mishra SK, Kang JH, Lee CW, Oh SH, Ryu JS, Bae YS, Kim HM: Midazolam induces cellular apoptosis in human cancer cells and inhibits tumor growth in xenograft mice. Mol Cells 2013; 36:219–26
25. Stevens MF, Werdehausen R, Gaza N, Hermanns H, Kremer D, Bauer I, Küry P, Hollmann MW, Braun S: Midazolam activates the intrinsic pathway of apoptosis independent of benzodiazepine and death receptor signaling. Reg Anesth Pain Med 2011; 36:343–9
26. Gargiulo S, Greco A, Gramanzini M, Esposito S, Affuso A, Brunetti A, Vesce G: Mice anesthesia, analgesia, and care, Part I: Anesthetic considerations in preclinical research. ILAR J 2012; 53:E55–69
27. Obeid EI, Conzen SD: The role of adrenergic signaling in breast cancer biology. Cancer Biomark 2013; 13:161–9
28. Bruzzone A, Piñero CP, Castillo LF, Sarappa MG, Rojas P, Lanari C, Lüthy IA: Alpha2-adrenoceptor action on cell proliferation and mammary tumour growth in mice. Br J Pharmacol 2008; 155:494–504
29. So EC, Lin YX, Tseng CH, Pan BS, Cheng KS, Wong KL, Hao LJ, Wang YK, Huang BM: Midazolam induces apoptosis in MA-10 mouse Leydig tumor cells through caspase activation and the involvement of MAPK signaling pathway. Onco Targets Ther 2014; 7:211–21
30. Scholzen T, Gerdes J: The Ki-67 protein: From the known and the unknown. J Cell Physiol 2000; 182:311–22
31. Whitwam JG, Amrein R: Pharmacology of flumazenil. Acta Anaesthesiol Scand Suppl 1995; 108:3–14
32. Sanders RD, Godlee A, Fujimori T, Goulding J, Xin G, Salek-Ardakani S, Snelgrove RJ, Ma D, Maze M, Hussell T: Benzodiazepine augmented γ-amino-butyric acid signaling increases mortality from pneumonia in mice. Crit Care Med 2013; 41:1627–36
33. Lopez J, Tait SW: Mitochondrial apoptosis: Killing cancer using the enemy within. Br J Cancer 2015; 112:957–62
34. Liou G, Storz P: Reactive oxygen species in cancer. Free Radic Res 2010; 44:10.3109/10715761003667554
35. Wong RSY: Apoptosis in cancer: From pathogenesis to treatment. J Exp Clin Cancer Res 2011; 30:87
36. Storz P: Reactive oxygen species in tumor progression. Front Biosci 2005; 10:1881–96
37. Hampton MB, Orrenius S: Dual regulation of caspase activity by hydrogen peroxide: Implications for apoptosis. FEBS Lett 1997; 414:552–6
38. Ozben T: Oxidative stress and apoptosis: Impact on cancer therapy. J Pharm Sci 2007; 96:2181–96
39. Cadenas E: Mitochondrial free radical production and cell signaling. Mol Aspects Med 2004; 25:17–26
40. Li PF, Dietz R, von Harsdorf R: p53 regulates mitochondrial membrane potential through reactive oxygen species and induces cytochrome c-independent apoptosis blocked by Bcl-2. EMBO J 1999; 18:6027–36
41. Gottlieb E, Vander Heiden MG, Thompson CB: Bcl-x(L) prevents the initial decrease in mitochondrial membrane potential and subsequent reactive oxygen species production during tumor necrosis factor alpha-induced apoptosis. Mol Cell Biol 2000; 20:5680–9
42. Halestrap AP: The mitochondrial permeability transition: Its molecular mechanism and role in reperfusion injury. Biochem Soc Symp 1999; 66:181–203
43. Crompton M: The mitochondrial permeability transition pore and its role in cell death. Biochem J 1999; 341 (Pt 2):233–49
44. Ravagnan L, Roumier T, Kroemer G: Mitochondria, the killer organelles and their weapons. J Cell Physiol 2002; 192:131–7
45. Patterson SD, Spahr CS, Daugas E, Susin SA, Irinopoulou T, Koehler C, Kroemer G: Mass spectrometric identification of proteins released from mitochondria undergoing permeability transition. Cell Death Differ 2000; 7:137–44
46. Castedo M, Perfettini JL, Kroemer G: Mitochondrial apoptosis and the peripheral benzodiazepine receptor: A novel target for viral and pharmacological manipulation. J Exp Med 2002; 196:1121–5
47. Strasser A, Harris AW, Bath ML, Cory S: Novel primitive lymphoid tumours induced in transgenic mice by cooperation between myc and bcl-2. Nature 1990; 348:331–3
48. Albarrán Juárez J, Gilsbach R, P Piekorz,Roland, Pexa K, Beetz N, Schneider J, Nürnberg B, Birnbaumer L, Hein L: Modulation of 2-adrenoceptor functions by heterotrimeric Gαi protein isoforms. J Pharmacol Exp Ther 2009; 331:35–44
49. Liu P, Cheng H, Roberts TM, Zhao JJ: Targeting the phosphoinositide 3-kinase pathway in cancer. Nat Rev Drug Discov 2009; 8:627–44
50. Wullschleger S, Loewith R, Hall MN: TOR signaling in growth and metabolism. Cell 2006; 124:471–84

51. Zhang M, Zhou X, Gao J, Wang K, Cui J: PI3K/Akt/mTOR pathway participates in neuroprotection by dexmedetomidine inhibits neuronic autophagy following traumatic brain injury in rats. Int J Res Med Sci 2017; 2:1569–75
52. Dou Y, Li Y, Chen J, Wu S, Xiao X, Xie S, Tang L, Yan M, Wang Y, Lin J, Zhu W, Yan G: Inhibition of cancer cell proliferation by midazolam by targeting transient receptor potential melastatin 7. Oncol Lett 2013; 5:1010–6
53. Weerink MAS, Struys MMRF, Hannivoort LN, Barends CRM, Absalom AR, Colin P: Clinical pharmacokinetics and pharmacodynamics of dexmedetomidine. Clin Pharmacokinet 2017; 56:893–913
54. Khan ZP, Munday IT, Jones RM, Thornton C, Mant TG, Amin D: Effects of dexmedetomidine on isoflurane requirements in healthy volunteers. 1: Pharmacodynamic and pharmacokinetic interactions. Br J Anaesth 1999; 83:372–80
55. Schwagmeier R, Alincic S, Striebel HW: Midazolam pharmacokinetics following intravenous and buccal administration. Br J Clin Pharmacol 1998; 46:203–6